Characterization of severe acute respiratory syndrome-associated coronavirus (SARS-CoV) spike glycoprotein-mediated viral entry

Graham Simmons, Jacqueline D. Reeves, Andrew J. Rennekamp, Sean M. Amberg, Andrew J. Piefer, and Paul Bates*

Department of Microbiology, University of Pennsylvania School of Medicine, 225 Johnson Pavilion, 3610 Hamilton Walk, Philadelphia, PA 19104

Edited by Peter S. Kim, Merck Research Laboratories, West Point, PA, and approved January 6, 2004 (received for review October 6, 2003)

Severe acute respiratory syndrome-associated coronavirus (SARS-CoV) is a rapidly emerging pathogen with potentially serious consequences for public health. Here we describe conditions that result not only in the efficient expression of the SARS-CoV spike (S) protein on the surface of cells, but in its incorporation into lentiviral particles that can be used to transduce cells in an S glycoprotein-dependent manner. We found that although some primate cell lines, including Vero E6, 293T and Huh-7 cells, could be efficiently transduced by SARS-CoV S glycoprotein pseudoviruses, other cells lines were either resistant or very poorly permissive to virus entry. Infection by pseudovirions could be inhibited by several lysosomotropic agents, suggesting a requirement for acidification of endosomes for efficient S-mediated viral entry. In addition, we were able to develop a cell–cell fusion assay that could be used to monitor S glycoprotein-dependent membrane fusion. Although proteolysis did not enhance the infectivity of cell-free pseudovirions, trypsin activation is required for cell–cell fusion. Additionally, there was no apparent pH requirement for S glycoprotein-mediated cell–cell fusion. Together, these studies describe important tools that can be used to study SARS-CoV S glycoprotein structure and function, including approaches that can be used to identify inhibitors of the entry of SARS-CoV into target cells.

Severe acute respiratory syndrome (SARS) is a contagious atypical pneumonia with a high mortality rate (1, 2). Recently, a previously uncharacterized virus, termed SARS-associated coronavirus (SARS-CoV), was isolated from SARS patients (3, 4) and demonstrated to cause disease in infected nonhuman primates (5). The coronaviruses are a diverse group of enveloped positive-strand RNA viruses that can cause respiratory, enteric, and neurologic diseases in their host species. Phylogenetic analysis reveals four groups, with the two previously identified human coronaviruses, 229E and OC43, falling in groups 1 and 2, respectively, and SARS-CoV forming a unique group, group 4 (6).

Coronaviruses, like other enveloped viruses, enter target cells by inducing fusion between viral and cellular membranes. This is mediated by a viral fusion protein termed spike or S protein. The S protein of a prototypical coronavirus, mouse hepatitis virus (MHV), is often cleaved posttranslationally into a heterodimer consisting of an extracellular receptor binding subunit, S1, and a membrane-anchored subunit, S2, responsible for mediating membrane fusion. Binding of S1 to its cellular receptor (CEACAM1) induces conformational changes in the S1/S2 complex (7), leading to viral entry. Although there is only 20–27% amino acid identity between SARS-CoV encoded S protein and those of the other coronavirus family members, a number of features are conserved, particularly in S2 (6). Additionally, SARS-CoV S contains 23 predicted N-linked glycosylation sites (6), of which at least 12 appear to be used (8).

To analyze the function of viral surface glycoproteins in isolation from postentry events and to increase the safety of studies on human pathogens, retroviral cores can be used to pseudotype surface glycoproteins such that viral entry is mediated by the glycoprotein in a specific manner. Glycoproteins from many viral families, including filoviruses, rhabdoviruses, bunyaviruses and flaviviruses, have been successfully pseudotyped into retroviral virions (9–11). Importantly, pseudovirions are also useful tools for rapid and quantitative analysis of potential neutralizing antibodies and inhibitors of viral entry. To date, no coronavirus pseudotypes have been described, although the presence of S at the cell surface suggests their feasibility.

To analyze the structure and function of the S protein from the SARS-associated coronavirus, we developed systems that not only resulted in the efficient expression of S protein at the cell surface, but made the production of SARS-CoV pseudotyped retroviruses and the development of a cell–cell fusion assay possible as well. These assays were used to characterize the mode of entry used by SARS-CoV and to assess the likely breadth of SARS-CoV receptor expression on primate cell lines as determined by the capacity of S to mediate entry.

Materials and Methods

Plasmids and Cell Lines. SARS-CoV (Urbani strain) RNA from pelleted infected Vero E6 cell supernatant was kindly provided by Paul Rota (Centers for Disease Control, Atlanta). Synthesis of cDNA was performed by using an oligonucleotide complementary to the 3′ end of the S gene (5′-CCGCGGTGTGTAATGTAATTTGAC-3′). SARS-CoV S was initially amplified by using the forward primer 5′-GCTAGCACCatgTTTATTTTCTTATTATTTC-3′ and the reverse primer described above to give S without a stop codon. Further subcloning into pCDNA6/V5-His (Invitrogen) resulted in S with a C-terminal V5/His tag. Identity to the published sequence (GenBank accession no. AY278741) was confirmed by sequencing. Subsequently, S/V5 was subcloned into pCAGGS-MCS or S was amplified from cDNA with the above forward primer together with the reverse primer 5′-AGCTAGCTTATGTGTAATGTAATTTG-3′ and cloned directly into pCAGGS-MCS to give full-length untagged S.

The HIV gag/pol construct, pΔR8.2, and the β-galactosidase (β-gal) reporter construct, pHX′-CMVLacZWP, have been described (12, 13). A luciferase (luc) reporter construct was made by replacing *lacZ* in pHR′-CMVLacZ (12) with firefly luc. Plasmids expressing Ebola GPΔmuc, vesicular stomatitis virus (VSV)-G, and hemagglutinin (HA) have been described (14).

All cell lines were cultured in DMEM supplemented with 10% FBS and penicillin/streptomycin (15 units/ml).

Expression of S Protein. 293T cells were transfected by using calcium phosphate and cultured for 40 h before cell lysates were

This paper was submitted directly (Track II) to the PNAS office.

Abbreviations: SARS, severe acute respiratory syndrome; SARS-CoV, SARS-associated coronavirus; S, spike protein; MHV, mouse hepatitis virus; β-gal, β-galactosidase; HA, hemagglutinin; luc, luciferase; CMV, cytomegalovirus; FFU, focus-forming unit; VSV, vesicular stomatitis virus.

*To whom correspondence should be addressed. E-mail: pbates@mail.med.upenn.edu.

www.pnas.org/cgi/doi/10.1073/pnas.0306446101

made by using M-Per detergent (Pierce) and analyzed by SDS/PAGE followed by Western blotting and detection with an anti-V5 antibody (Invitrogen). For T7 polymerase-driven expression, cells were exposed to vaccinia virus vTF1.1 (15) at a multiplicity of infection of five 1 h before transfection, washed, and transfected with pCDNA6 S/V5-His, and cultured in the presence of Rifampicin for 18 h at 32°C before analysis.

Pseudotype Production. 293T cells were transfected with 20 μg of viral envelope expression plasmid plus 8 μg of pΔR8.2 and 6.5 μg of HIV reporter per 10-cm dish by using calcium phosphate. The next day, expression was induced with sodium butyrate (10 mM) for 4 h before washing once. Forty hours after transfection, supernatant was harvested and filtered through a 0.45-μm-pore-size screen. Preliminary tests indicated that neither freezing at −80°C nor short-term storage at 4°C dramatically affected viral titers.

Reflotation of Particles. Virions from cells cotransfected with pCAGGS S/V5-His and pΔR8.2 were filtered through a 0.45-μm-pore-size screen, pelleted for 1 h at 40,000 rpm through a 20% sucrose cushion in a SW41 rotor, and resuspended in sucrose at a final concentration of 60%. After overlayering with 50% and 10% sucrose steps, particles were refloated by centrifugation in a SW50 rotor at 40,000 rpm for 4 h. Fractions (700 μl), such that the 50/10% interface would be contained within the first fraction, were collected from the top to the bottom of the gradient and analyzed by SDS/PAGE for the V5 epitope.

Pseudovirion Infection. Pseudovirions were titrated on various cell types seeded at 4–6 $\times$ 10^4 in 24-well plates by using 500 μl of media containing varying amounts of viral supernatant to spin infect at 1,200 $\times$ *g* for 120 min at 4°C. After a further 2-h incubation at 37°C, 1.5 ml of fresh medium was added and cells were incubated for 40 h. Cells were then fixed in 2% paraformaldehyde and stained for β-gal expression as described (11).

Neutralization of pseudovirions was performed by using sera from a convalescent SARS patient 18 days after onset of symptoms (kindly supplied by William Bellini, Centers for Disease Control). Sera was inactivated at 50°C, serially diluted, and mixed with luc reporter pseudovirions at a 1:1 ratio and incubated for 45 min at room temperature before addition of 50 μl to 293T cells seeded at 2 $\times$ 10^4 cells per well in 96-well plates. After spin infection, cells were incubated for 2 h at 37°C, washed twice, and incubated for 40 h. Luc activity was assayed in cell lysates as per manufacturer's instructions (Promega), and read on a Wallac luminometer. HIV(VSV-G) and HIV(S) luc pseudovirions were pretitrated on 293T cells to ensure similar input levels of viruses.

Lysosomotropic Agents. Cells were incubated with serial dilutions of Balfilomycin A, chloroquine, or NH_4Cl 1 h before and during spin infection with virus at a multiplicity of infection of ≈0.02. The agent was included in the medium for 18 h after infection, before replacement with fresh medium and assaying for transduction 40 h after infection.

Acid Inactivation. Pseudovirions were prepared as above. For HIV(HA) virions, producer cells were treated with neuraminidase (25 milliunits/ml) both 18 and 2 h before harvesting the supernatant. Supernatants were ultracentrifuge-concentrated at 40,000 rpm in a SW41 rotor for 45 min at 4°C and resuspended in PBS. HA virions were treated with L-1-tosylamide-2-phenylethyl chloromethyl ketone-treated (TPCK) trypsin (15 μg/ml) for 14 min at 37°C before inactivation with soybean trypsin inhibitor (50 μg/ml). HIV(S), HIV(HA), or HIV-(VSV-G) pseudovirions encoding luc were preincubated for 30 min at 37°C in medium at pH 7.5 or 5.0 before neutralization with 25 mM Hepes-buffered DMEM (pH 7.5) and spin infection on Vero E6 cells.

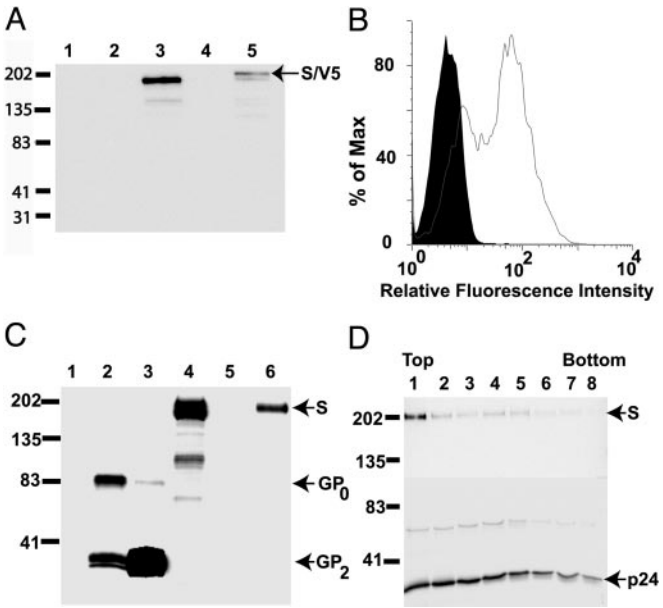

Fig. 1. Expression and incorporation of SARS-CoV S into retroviral particles. (*A*) Detection of V5 epitope in transfected 293T cells. Lanes 1 and 4, mock transfected cells; lanes 2 and 3, cells transfected with pCDNA6 S/V5-His; lane 5, pCAGGS S/V5-His expressing cells. Lanes 3 and 4 were coinfected with Vaccinia expressing T7 pol. Markers represent kDa. (*B*) Surface expression of S. Shown are 293T cells transfected with empty vector (filled histogram) or pCAGGS S (open histogram) were analyzed, using human convalescent sera (1/200) and an anti-human Ig/FITC conjugate. (*C*) Release and cleavage of S/V5-His or Ebola GP/V5-His in transfected 293T cells. Lane 1, mock; lanes 2 (cell lysate) and 3 (supernatant), pCAGGS Ebola GPΔmuc/V5-His; lanes 4 (cell lysate) and 5 (supernatant), pCAGGS S/V5-His; lane 6, cell supernatant of cells cotransfected with pCAGGS S/V5-His and HIV gag/pol. (*D*) Reflotation of particles analyzed for V5 (*Upper*) or HIV p24 (*Lower*).

Cell–Cell Fusion. 293T effector cells transfected with 2 μg of GFP and 6 μg of pCAGGS S or control vector 2 days before assaying were detached with EDTA and mock or TPCK trypsin (15 μg/ml) treated in suspension for 15 min at 37°C before inactivation with soybean trypsin inhibitor. Target Vero E6 cells were prelabeled with 5-(and 6)-([{4-chloromethyl}benzoyl] amino)tetramethylrhodamine (CMTMR) (Molecular Probes) as per the manufacturer's instructions. Effector cells were then incubated with targets for 1 h at 37°C, pulsed for 15 min with pH 5.0 or 7.5 medium at 37°C, then returned to pH 7.5 medium. Cells were incubated and observed by fluorescence microscopy for cell–cell fusion.

Results

Expression of SARS-CoV S. S glycoprotein was cloned into pCDNA6 with a C-terminal V5-His epitope tag that could be used to monitor protein expression. However, the S glycoprotein was not detected in the lysates of 293T cells transiently transfected with the pCDNA6 construct (Fig. 1*A*, lane 2). Because expression from pCDNA6 can be driven either by the cytomegalovirus (CMV) or T7 polymerase promoters, we transfected 293T cells with the S glycoprotein construct after infection with a recombinant vaccinia virus vector that expresses T7 polymerase (15). Western blot analysis of the resulting cell lysates revealed the expression of a V5-tagged protein of ≈200 kDa (Fig. 1*A*, lane 3). In addition, a fainter band of ≈140 kDa, the predicted size of S based on amino acid composition (8), was

MICROBIOLOGY

detected. This may represent unglycosylated S protein that could result from overexpression induced by the vaccinia virus system.

Although the vaccinia virus system made it possible to express S at detectable levels, this approach generally fails to result in the efficient production of virus pseudotypes. Because expression of S via the CMV promoter was below the limits of detection, we subcloned S/V5-His and full-length untagged S into pCAGGS, a mammalian expression vector under the control of a chicken β-actin promoter that, in the past, has proved useful for the efficient expression of RNA virus glycoproteins (16–18). Transient expression in 293T cells by using pCAGGS S/V5-His resulted in detectable expression of S/V5-His in cell lysates (Fig. 1*A*, lane 5). It is not clear why pCAGGS was more efficient at driving S expression compared to pCDNA6, but other CMV promoter-containing vectors also failed to give detectable levels of S expression (data not shown).

The pCAGGS expressed S/V5-His glycoprotein ran as a tightly spaced doublet with the weaker, lower band corresponding to the size of S/V5-His observed on Vaccinia/T7 expression (Fig. 1*A*, lane 3 vs. lane 5). The more slowly migrating band may result from differential carbohydrate processing of S. When greater amounts of cell lysate were analyzed by SDS/PAGE and Western blot, an additional lower molecular mass band of $\approx$100 kDa was detected (Fig. 1*C*, lane 4). It is possible that this represents S2, the membrane-bound subunit of S. Indeed, the S2 protein of MHV exhibits a similar mobility (19). The development of S1 and S2 specific antibodies will be needed to more fully explore SARS-CoV S glycoprotein processing. To determine whether S protein was expressed on the surface of transfected 293T cells, we used convalescent SARS patient sera to detect S glycoproteins by live-cell flow cytometry (Fig. 1*B*). Cells transfected with pCAGGS S, but not empty vector, demonstrated a sizable population of cells reacting with the sera, indicative of efficient surface expression of S. No reactivity to S-expressing cells was observed with control human sera (data not shown).

Incorporation of S into Retroviral Particles. Expression of S/V5-His alone did not result in release of detectable protein into the cell supernatant (Fig. 1*C*, lane 5). This is in contrast to Ebola GP, which is released in membrane vesicles when expressed at high levels in cells (Fig. 1*C* and ref. 20). However, coexpression of SARS-CoV S with HIV gag/pol led to easily detectable V5-tagged S in the supernatant, suggesting incorporation of S/V5-His into budding HIV particles (Fig. 1*C*, lane 6). Only the full-length S glycoprotein was detected in the supernatant. The putative S2 protein subunit noted in 293T cell lysates was either not incorporated into virus particles or was present at levels below the limit of detection. However, it should be noted that only a small fraction of S protein was cleaved in 293T cells. Whether cleavage of S occurs more efficiently in other cell types remains to be determined. Finally, to determine whether S protein detected in the media of cells transfected with both pCAGGS S/V5-His and the HIV gag/pol construct was, in fact, incorporated into pseudovirions, we subjected virions to flotation gradient sedimentation. Under these conditions, the HIV p24 gag protein floats to the top of a sucrose step gradient (10/50/60%) because of the presence of the lipid bilayer that surrounds the virus particle (Fig. 1*D*). The S/V5-His glycoprotein was also recovered at the top of the gradient, indicating that it was, in fact, incorporated into p24-containing virus particles (Fig. 1*D*).

S Glycoprotein-Mediated Viral Entry. The ability to incorporate S glycoprotein into particles potentiates the use of lentiviral vectors, with their wide array of reporter systems, such as β-gal, luc, and GFP, for analyzing S-mediated entry into cells. Vero E6, an African green monkey kidney cell line and a known target for SARS-CoV replication (3), were challenged under a variety of

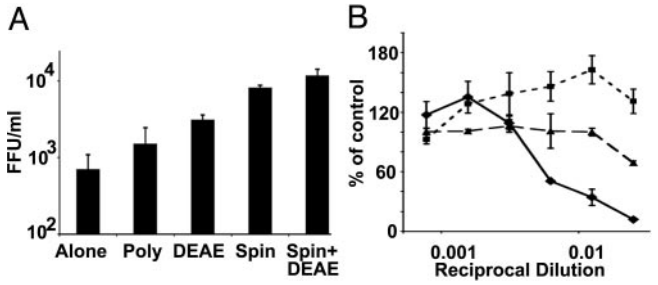

Fig. 2. Optimization and neutralization of HIV(S) pseudovirions. (*A*) Titers of HIV(S) pseudovirions encoding β-gal on Vero E6 cells calculated as focus-forming units per ml (FFU/ml). Cells were incubated for 18 h at 37°C with 250 μl of diluted virus supernatants (alone), or with polybrene (poly) or DEAE-dextran (DEAE) at 3.2 μg/ml. Alternatively, cells were spin infected (Spin) with 500 μl of diluted virus supernatants or together with DEAE-dextran at 3.2 μg/ml (Spin + DEAE). Values are means of quadruplet wells $\pm$ SD. (*B*) Luc-encoding HIV(S) was preincubated with serial dilutions of 18-day convalescent patient serum (solid line, diamonds) or normal human serum (dotted line, squares). Results are presented as a percentage of no sera (3.2×10^5 relative light units) and represent the means of triplicate wells $\pm$ SD. HIV(VSV-G) was also preincubated with patient serum (dashed line, triangles). The experiment is representative of two experiments.

conditions with pseudovirions encoding β-gal and bearing untagged S to avoid potential interference from a C-terminal epitope tag [HIV(S) particles]. Whereas particles produced in the absence of viral glycoprotein resulted in titers of <4 focus-forming units/ml (FFU/ml) under any conditions, HIV(S) pseudovirions routinely gave titers of 7.0×10^2 FFU/ml (Fig. 2*A*). Although relatively low, this titer partially reflects the poor ability of HIV to replicate in many nonhuman primate cells (21). Indeed, HIV(VSV-G), which displays a very broad tropism (11), only produced titers on Vero E6 cells of 8.3×10^4, compared to 1.1×10^7 FFU/ml on 293T cells. Various nonspecific mechanisms commonly used to enhance viral binding, including DEAE dextran and spin infection, increased the titer of HIV(S) up to as much as 1.2×10^4 FFU/ml on Vero E6 cells. HIV(S) virions also gave a titer of 6.5×10^4 FFU/ml on 293T cells by using spin infection alone (Table 1). S-mediated transduction of 293T cells could be inhibited by the neutralizing ability of convalescent SARS patient sera, but not control human sera, on luc-encoding HIV(S) pseudovirions (Fig. 2*B*), with a 1 in 40 dilution reducing transduction by >90% compared to the no-antibody control. In addition, the SARS patient sera did not neutralize VSV-G-mediated transduction of 293T cells. Thus, virus entry resulting from transduction of cells with HIV(S) particles was specific, and depended on the presence of the SARS-CoV S glycoprotein.

The HIV(S) pseudovirions were used to test a diverse panel

Table 1. Transduction of primate cell lines

	FFU/ml	
Cell type	HIV (S)	HIV (VSV-G)
293T (Hu)	6.5×10^4	1.1×10^7
A549 (Hu)	19	3.6×10^5
HeLa (Hu)	42	2.2×10^5
HOS (Hu)	<8	5.3×10^5
HT1080 (Hu)	1.0×10^3	1.1×10^7
Huh-7 (Hu)	1.8×10^3	5.2×10^6
K562 (Hu)	<8	1.0×10^5
NP2 (Hu)	12	2.6×10^6
COS (AGM)	11	4.4×10^4
Vero (AGM)	8.1×10^3	8.3×10^4

Hu, human; AGM, African green monkey.

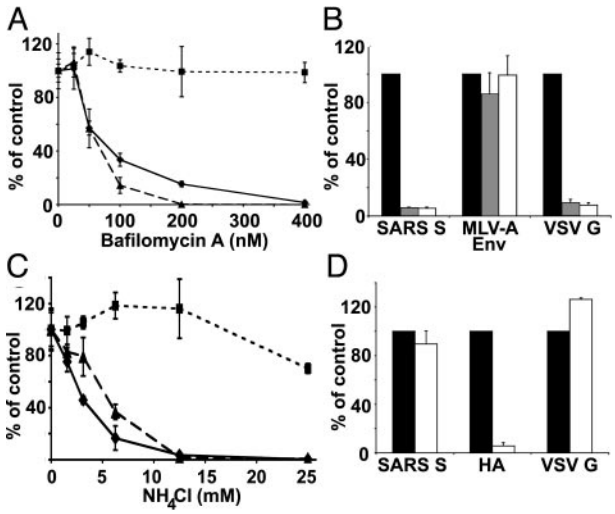

Fig. 3. Effects of lysosomotropic agents on HIV(S) transduction. (*A*) Bafilomycin A inhibition of Vero E6 transduction by HIV(S) encoding β-gal (solid line, diamonds), HIV(VSV-G) (dashed line, triangles), or HIV(MLV-A env) (dotted line, squares). Results are expressed as a percentage of no drug and represent the means of triplicate wells ± SD. The experiment is representative of two experiments. (*B*) Inhibition of Vero E6 transduction by NH_4Cl (shaded bars) or chloroquine (open bars). Results are a percentage of no drug control (filled bars) and are the means of quadruplet wells ± SD. (*C*) NH_4Cl inhibition of 293T transduction by HIV(S) encoding β-gal (solid line, diamonds), HIV(VSV-G) (dashed line, triangles), or HIV(MLV-A env) (dotted line, squares). Results are expressed as a percentage of no NH_4Cl control and represent the means of quadruplet wells ± SD. This experiment is representative of three experiments. (*D*) Pretreatment of pseudovirions with pH 7.5 (filled bars) or 5.0 (open bars). Results are presented as a percentage of the pH 7.5 results (6.9×10^3, 1.6×10^4, and 2.2×10^4 relative light units for S, HA, and VSV-G, respectively) and are the means of triplicate wells ± SD. This experiment is representative of two experiments.

of cell types from different tissues for S-mediated viral entry (Table 1). In addition to the embryonal kidney cell line, 293T, the only other human cell lines to be markedly transduced by HIV(S) were the hepatocellular carcinoma line Huh-7 and the fibrosarcoma line HT1080 (Table 1). Several cell lines, such as an osteosarcoma line (HOS), were not infectable, despite efficient transduction by VSV-G. Several other cell lines, including a lung carcinoma line (A549) and the epithelial cell line HeLa, exhibited a low level of transduction that was consistently above background. Although Vero E6 cells, the prototypic cell line for culturing SARS-CoV (3), were transducable by HIV(S), two other African green monkey kidney cell lines, COS-7 and CV-1, did not appear to be infected, despite similar levels of VSV-G-mediated transduction (Table 1 and data not shown). Preliminary data also suggested that a range of nonprimate cell lines, including murine, feline, and avian cells, were not transduced efficiently by HIV(S). However, higher-titer pseudovirions will have to be developed to classify these lines as truly refractory to SARS-CoV S glycoprotein-mediated virus entry.

Sensitivity to Lysosomotropic Compounds. The sensitivity of HIV(S) pseudovirions to lysosomotropic agents was assessed on Vero E6 and 293T cells (Fig. 3). Bafilomycin A, an inhibitor of vacuolar H^+-ATPases responsible for acidifying endosomes, inhibited transduction of Vero E6 cells by HIV(S), although slightly higher concentrations were required to fully inhibit transduction than for the pH-dependent viral envelope, VSV-G, which undergoes fusion-inducing conformational changes at mildly acidic pH values (Fig. 3*A*). In contrast, the pH-independent envelope glycoprotein, amphotropic-MLV Env (22), was unaffected even by high concentrations of Bafilomycin A, indicating that the inhibitory effects of Bafilomycin A did not result from postentry inhibition of HIV core replication. Likewise, the acidotropic weak bases ammonium chloride (NH_4Cl) and chloroquine also inhibited transduction of Vero E6 cells by HIV(S) and HIV(VSV-G), but not HIV(MLV-A env) (Fig. 3*B*). Inhibition by NH_4Cl of HIV(S) transduction was also observed on 293T cells (Fig. 3*C*).

Many, although not all, pH-dependent viral surface glycoproteins, such as influenza HA, are inactivated by pretreatment with low pH before contact with cells because of the induction of premature, irreversible conformational rearrangements in the glycoprotein (23). The G glycoprotein of VSV is notable for undergoing reversible acid pH-induced conformational changes, and thus is not inactivated by pretreatment at acid pH (24). To determine whether the SARS-CoV S glycoprotein could be inactivated by low pH treatment, luc-encoding HIV(S) pseudovirions, along with HIV(HA) and HIV(VSV-G), were incubated at 37°C for 30 min at pH 5.0 or 7.5 before neutralization and spin infection onto Vero E6 cells. Unlike HA-mediated transduction, HIV(S) transduction of cells was not significantly reduced by low pH pretreatment (Fig. 3*D*).

S-Mediated Cell–Cell Fusion. Having shown that the SARS-CoV S glycoprotein can be transiently expressed on the cell surface, we sought to further study its membrane fusion activity through the development of a cell–cell fusion assay. The S glycoprotein was expressed in 293T cells because this cell line allowed surface expression of S and supported the production of infectious pseudovirions. The transfected 293T cells were then mixed with Vero E6 cells, because these cells support infection by replication-competent SARS virus and must therefore possess any needed cellular receptors. To monitor fusion, GFP was coexpressed along with the S glycoprotein in 293T cells, whereas the Vero E6 cells were prestained with an orange cytoplasmic dye (Fig. 4). We found that little or no cell–cell fusion occurred at either pH 7.5 or pH 5.0. In contrast, cells expressing VSV-G fused with Vero E6 cells efficiently at low pH (Fig. 5, which is published as supporting information on the PNAS web site). However, because cleavage of S protein appears to occur inefficiently in 293T cells and uncleaved protein may inhibit fusion in a transdominant fashion, we treated 293T cells expressing the S glycoprotein with low concentrations of trypsin. Similar trypsin treatment is needed to activate the membrane fusion potential of many influenza HA strains (25). We found that specific, although inefficient, cell–cell fusion occurred after brief trypsin treatment of cells expressing S at both pH 7.5 and 5.0 (Figs. 4 and 5). An average of 10 syncytia (judged as dual green and red stained giant multinucleated cells containing four or more nuclei) per well were observed at pH 5 compared to 14 per well at pH 7. In the absence of trypsin treatment, no syncytia were observed at either neutral or acid pH. Thus, for cell–cell fusion at least, a low pH pulse does not appear to be required for S to mediate membrane fusion.

Discussion

SARS-CoV has the potential to become a highly important emerging pathogen. However, very little is known about the biology of this coronavirus, although its similarity to other coronaviruses suggests general principles that may govern its biological activities. We have successfully exploited the cell surface expression of SARS-CoV S protein in transfected cells to produce lentiviral particles that are able to transduce cells in an S glycoprotein-mediated manner. Although many cell lines were refractory to pseudovirions bearing SARS-CoV S, the primate cell lines Vero E6, 293T, HT1080, and Huh-7 were efficiently transduced.

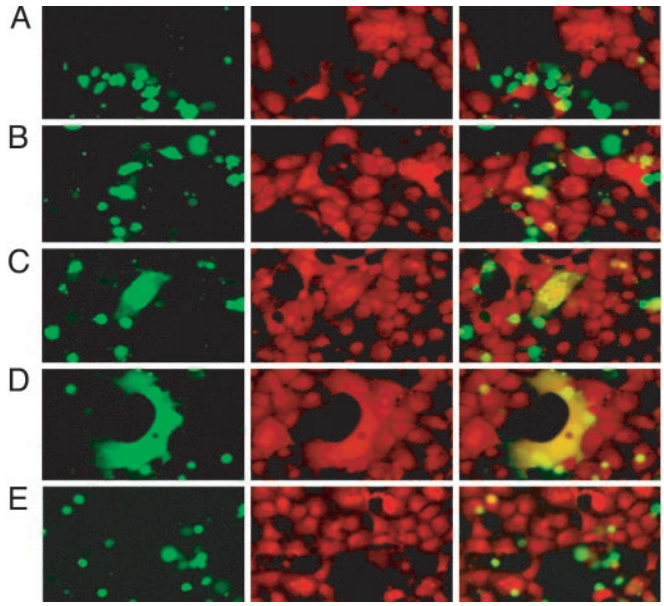

Fig. 4. Cell–cell fusion mediated by SARS-CoV S. S- and GFP-expressing 293T effector cells incubated with CMTMR-labeled Vero E6 target cells are shown. Effectors were either used directly (*A* and *B*) or pretreated with TPCK trypsin (*C* and *D*). After 1 h, cells were pulsed with pH 7.5 (*A* and *C*) or pH 5.0 (*B* and *D*) medium. Control cells expressing GFP and empty vector alone were pulsed with pH 5.0 (*E*). Other conditions for GFP and empty vector alone were all negative for fusion (data not shown). This experiment is representative of three experiments.

To mediate membrane fusion and entry, viral glycoproteins are triggered to undergo a series of conformational rearrangements forming several intermediate structures (26). Binding to a cell surface receptor(s) is sufficient to induce these conformational changes in pH-independent viruses such as HIV. However, other viruses, as exemplified by influenza, require a low pH instead of, or in addition to, receptor binding to trigger fusion. A low pH environment is encountered upon trafficking of the virus to acidified endosomal organelles via endocytosis (27).

Many coronaviruses mediate cell–cell fusion at neutral pH (28). However, inhibitors of endosomal acidification can block coronavirus replication, either because of effects on coronaviral glycoproteins or possibly effects on postentry steps of the viral life cycle (29). Thus, to study S-mediated entry in isolation, HIV(S) pseudovirions were used. These pseudovirions infect cells in an S-dependent manner, as evidenced by neutralization with SARS convalescent patient sera. We observed potent inhibition of SARS-CoV S-mediated transduction by two different classes of lysosomotropic agents in multiple cell lines, strongly suggesting that SARS-CoV glycoprotein requires acidification of endosomes for entry.

The lack of sensitivity of the SARS-CoV S glycoprotein to low pH pretreatment despite its sensitivity to lysosomotropic agents could result from one of at least four possibilities: the pH-induced conformational changes in S are reversible in a manner similar to VSV-G protein (24); triggering of S by receptor interactions is required before low pH can induce further rearrangements, as has been suggested for the avian sarcoma/leukosis virus (ASLV) Env glycoprotein (30); the S glycoprotein undergoes a processing event, such as cleavage, in endosomes that is a prerequisite for acid activation, as has been documented for influenza infection of Madin–Darby bovine kidney (MDBK) cells (31); or low pH is not required for infection, with sensitivity to lysosomotropic agents resulting from a mechanism other than ablation of intracellular pH gradients. Distinguishing between these possibilities will require the development of additional SARS-specific reagents and assays.

The glycoproteins of many enveloped viruses are cleaved by proteases into surface- and membrane-bound subunits. For example, cleavage at a monobasic site within HA (to give HA1 and HA2) is required for influenza virus infectivity (25). Most strains of MHV S contain a typical furin-like protease cleavage site. Although this site is absent in SARS-CoV S, the corresponding area includes two single basic amino acids, potential targets for trypsin-like cleavage. In agreement with published reports characterizing glycoprotein in SARS-CoV produced from cultured cells (8), we were unable to detect cleavage of incorporated SARS-CoV S protein in 293T produced HIV(S) pseudovirions, suggesting that these sites are not efficiently used during virus production. However, treatment of such virions with exogenous trypsin resulted in a protein species with a mobility of approximately the size of that predicted for S2 (Fig. 6, which is published as supporting information on the PNAS web site). Also, trypsin cleavage was a prerequisite for detectable S protein-mediated cell–cell fusion. Thus, SARS-CoV S may be cleaved after virion release, either in the cell supernatant or by the target cell. In preliminary experiments, trypsin cleavage of S on virions before infection of cells reduced infectivity (data not shown). This finding is in keeping with the hypothesis that cleavage may occur on or in the target cell. Indeed, in certain cell lines, cleavage of HA is postulated to occur by endosomal proteases (31). It is possible that the function of these proteases is pH-dependent or that trafficking of the incoming virus to the site of protease cleavage requires low pH, thus explaining the sensitivity of HIV(S) pseudovirions to lysosomotropic agents. Alternatively, SARS-CoV S may be able to mediate infection in a pH-dependent manner in the absence of cleavage, but trypsin-mediated cleavage may sufficiently reduce the threshold for triggering of conformational changes such that cell–cell fusion occurs at neutral pH. This would explain the dichotomy between pH-independent cell–cell fusion and the sensitivity of pseudovirions to lysosomotropic agents. A similar situation may be seen with MHV where replication in hepatocytes and glial cells does not result in efficient S protein cleavage (32), perhaps because of the absence of the correct proteases. Although virus continues to spread and infect in a cell-free manner, cell–cell fusion is not observed unless trypsin is added (32). It may be that differing requirements for cleavage might reflect differences in available receptor type or receptor density whereby SARS-CoV could only infect cells with low receptor when S is proteolytically processed, but in cells with high receptor density, S cleavage is not required. As has been suggested for influenza (33), a requirement for protease-mediated activation of envelope glycoproteins especially after virion release, may allow for the use of protease inhibitors as a potential antiviral therapeutic.

We describe here successful characterization of coronavirus S protein-mediated entry of lentiviral-based vectors. These pseudovirions will be useful tools in the study of SARS-CoV S structure/function, including the identification and evaluation of potential inhibitors and neutralizing antibodies of SARS-CoV entry.

We thank Paul Rota and William Bellini for reagents, Cassandra Jabara and Fang Hua Lee for technical assistance, and Robert Doms for advice and reading of the manuscript. This work was funded by National Institutes of Health (NIH) Grants RO1 AI43455 and CA76256. G.S. is supported by NIH Career Development Award A157172. J.D.R. is supported by American Foundation for AIDS Research Fellowship 106437-34-RFGN.

1. Lee, N., Hui, D., Wu, A., Chan, P., Cameron, P., Joynt, G. M., Ahuja, A., Yung, M. Y., Leung, C. B., To, K. F., *et al.* (2003) *N. Engl. J. Med.* **348,** 1986–1994.
2. Poutanen, S. M., Low, D. E., Henry, B., Finkelstein, S., Rose, D., Green, K., Tellier, R., Draker, R., Adachi, D., Ayers, M., *et al.* (2003) *N. Engl. J. Med.* **348,** 1995–2005.
3. Ksiazek, T. G., Erdman, D., Goldsmith, C. S., Zaki, S. R., Peret, T., Emery, S., Tong, S., Urbani, C., Comer, J. A., Lim, W., *et al.* (2003) *N. Engl. J. Med.* **348,** 1953–1966.
4. Peiris, J. S., Lai, S. T., Poon, L. L., Guan, Y., Yam, L. Y., Lim, W., Nicholls, J., Yee, W. K., Yan, W. W., Cheung, M. T., *et al.* (2003) *Lancet* **361,** 1319–1325.
5. Fouchier, R. A., Kuiken, T., Schutten, M., van Amerongen, G., van Doornum, G. J., van den Hoogen, B. G., Peiris, M., Lim, W., Stohr, K. & Osterhaus, A. D. (2003) *Nature* **423,** 240.
6. Rota, P. A., Oberste, M. S., Monroe, S. S., Nix, W. A., Campagnoli, R., Icenogle, J. P., Penaranda, S., Bankamp, B., Maher, K., Chen, M. H., *et al.* (2003) *Science* **300,** 1394–1399.
7. Zelus, B. D., Schickli, J. H., Blau, D. M., Weiss, S. R. & Holmes, K. V. (2003) *J. Virol.* **77,** 830–840.
8. Krokhin, O., Li, Y., Andonov, A., Feldmann, H., Flick, R., Jones, S., Stroeher, U., Bastien, N., Dasuri, K. V., Cheng, K., *et al.* (2003) *Mol. Cell Proteomics* **2,** 346–356.
9. Bartosch, B., Dubuisson, J. & Cosset, F. L. (2003) *J. Exp. Med.* **197,** 633–642.
10. Ma, M., Kersten, D. B., Kamrud, K. I., Wool-Lewis, R. J., Schmaljohn, C. & Gonzalez-Scarano, F. (1999) *Virus Res.* **64,** 23–32.
11. Wool-Lewis, R. J. & Bates, P. (1998) *J. Virol.* **72,** 3155–3160.
12. Naldini, L., Blomer, U., Gallay, P., Ory, D., Mulligan, R., Gage, F. H., Verma, I. M. & Trono, D. (1996) *Science* **272,** 263–267.
13. Watson, D. J., Kobinger, G. P., Passini, M. A., Wilson, J. M. & Wolfe, J. H. (2002) *Mol. Ther.* **5,** 528–537.
14. Simmons, G., Wool-Lewis, R. J., Baribaud, F., Netter, R. C. & Bates, P. (2002) *J. Virol.* **76,** 2518–2528.
15. Alexander, W. A., Moss, B. & Fuerst, T. R. (1992) *J. Virol.* **66,** 2934–2942.
16. Takada, A., Robison, C., Goto, H., Sanchez, A., Murti, K. G., Whitt, M. A. & Kawaoka, Y. (1997) *Proc. Natl. Acad. Sci. USA* **94,** 14764–14769.
17. Pekosz, A. & Lamb, R. A. (1999) *J. Virol.* **73,** 8808–8812.
18. Hsu, M., Zhang, J., Flint, M., Logvinoff, C., Cheng-Mayer, C., Rice, C. M. & McKeating, J. A. (2003) *Proc. Natl. Acad. Sci. USA* **100,** 7271–7276.
19. Sturman, L. S., Ricard, C. S. & Holmes, K. V. (1985) *J. Virol.* **56,** 904–911.
20. Volchkov, V. E., Volchkova, V. A., Slenczka, W., Klenk, H. D. & Feldmann, H. (1998) *Virology* **245,** 110–119.
21. Besnier, C., Takeuchi, Y. & Towers, G. (2002) *Proc. Natl. Acad. Sci. USA* **99,** 11920–11925.
22. McClure, M. O., Sommerfelt, M. A., Marsh, M. & Weiss, R. A. (1990) *J. Gen. Virol.* **71,** 767–773.
23. Boulay, F., Doms, R. W., Wilson, I. & Helenius, A. (1987) *EMBO J.* **6,** 2643–2650.
24. Doms, R. W., Keller, D. S., Helenius, A. & Balch, W. E. (1987) *J. Cell Biol.* **105,** 1957–1969.
25. Klenk, H. D., Rott, R., Orlich, M. & Blodorn, J. (1975) *Virology* **68,** 426–439.
26. Eckert, D. M. & Kim, P. S. (2001) *Annu. Rev. Biochem.* **70,** 777–810.
27. Marsh, M. & Pelchen-Matthews, A. (2000) *Traffic* **1,** 525–532.
28. Kooi, C., Cervin, M. & Anderson, R. (1991) *Virology* **180,** 108–119.
29. Nash, T. C. & Buchmeier, M. J. (1997) *Virology* **233,** 1–8.
30. Mothes, W., Boerger, A. L., Narayan, S., Cunningham, J. M. & Young, J. A. (2000) *Cell* **103,** 679–689.
31. Boycott, R., Klenk, H. D. & Ohuchi, M. (1994) *Virology* **203,** 313–319.
32. Hingley, S. T., Leparc-Goffart, I. & Weiss, S. R. (1998) *J. Virol.* **72,** 1606–1609.
33. Klenk, H. D. & Garten, W. (1994) *Trends Microbiol.* **2,** 39–43.